Subsidence monitoring within the Athens Basin (Greece) using space radar interferometric techniques

Is. Parcharidis[1], E. Lagios[2], V. Sakkas[2], D. Raucoules[3], D. Feurer[3], S. Le Mouelic[3], C. King[3], C. Carnec[3],
F. Novali[4], A. Ferretti[4], R. Capes[5], and G. Cooksley[5]

[1]*Harokopio University of Athens, Department of Geography, El. Venizelou 70, 17671 Athens, Greece*
[2]*Space Applications Research Unit in Geosciences, Laboratory of Geophysics, Department of Geophysics & Geothermics,
National Capodistrian University of Athens, Panepistimiopolis - Ilissia, 157 84 Athens, Greece*
[3]*BRGM, 3 avenue Guillemin, BP 6009, 45060 - Orléans cedex 2 - France*
[4]*Tele-Rilevamento-Europa, via Vittoria Colonna, 7, 20149 Milano, Italy*
[5]*NPA Group, Crockham Park, Edenbridge, Kent, TN8 6SR, U.K.*

The application of conventional SAR Interferometry (InSAR) together with the two techniques of sub-centimeter accuracy, the Stacking and the Permanent Scatterers (PS) Interferometry, were used to study the ground deformation in the broader area of Athens for the period 1992 to 2002. Using the Stacking interferometric method, 55 ERS-1&2 SAR scenes, between 1992 and 2002, were acquired producing 264 differential interferograms. Among these only 60 were finally selected as fulfilling certain criteria. The co-seismic deformation associated with the Athens Earthquake ($M_w = 5.9$, September 7, 1999) was excluded from the analytical procedure in an attempt to present results of only aseismic character. In total ground subsidence results of about 12 mm in the southern suburbs of Athens, but higher value of about 40 mm in the northern ones for the period 1992–2002. Based on the PS technique, a precise average annual deformation rate-map was generated for the period 1992–1999, ending just before the Athens earthquake event. Both circular and elongated-shape areas of subsidence are recognizable especially in the northern part of the Athens Basin (3–4 mm/yr), as well as at its southern part (1–3 mm/yr). In addition, a rate of 2–3 mm/yr is also yielded for some part of the Athens city center. Subsidence rates of 1–2 mm/yr are measured at the western part of the basin over an area of old mining activities, and around the newly built Syntagma Metro Station. The correlation of the observed deformation patterns with respect to the spatial distribution of water pumping, older mining activities, metro line tunneling and other local geological parameters is examined and discussed.

Key words: Athens Basin, subsidence, deformation monitoring, differential interferometry, stacking interferometry, Permanent Scatterers Interferometry.

1. Introduction

The results of ground displacement measurements, especially in urban areas, are outlined in this study based on advanced space application techniques. The ground subsidence being produced by many causes (e.g. subtraction of earth material by mining or tunneling, fluid pumping such as groundwater, oil, gas etc.) does not pose the type of hazards associated with sudden and catastrophic natural events like earthquakes. However, in urban areas, high vulnerability to the effects of subsidence is exhibited. Within urban areas, especially in those that are highly populated like the broader region of Athens, important projects and structures are concentrated (e.g. bridges, highways, underground life-lines pipes, metro), increasing thus the exposure to the hazard.

Measuring subsidence using ground-based techniques like levelling and geodetic surveys is not a new concept. However, new techniques were developed to measure subsidence in recent years. Repeat-pass space-borne Synthetic Aperture Radar (SAR) interferometry (InSAR) is a unique tool for large coverage (spatially continuous) surface deformation monitoring at low cost (Massonnet *et al.*, 1993; Zebker *et al.*, 1994), particularly for subsidence regardless of the causes (Fielding *et al.*, 1998; Galloway *et al.*, 1998; Wright and Stow, 1999; Carnec and Fabriol, 1999; Avallone *et al.*, 1999; Carnec and Delacourt, 2000; Strozzi *et al.*, 2001; Hoffmann *et al.*, 2001). Subsidence effects in urban areas generated by natural or anthropogenic causes have already been detected and reported using the conventional repeat-pass InSAR technique (Amelung *et al.*, 1999; Wegmüller *et al.*, 1999; Tesauro *et al.*, 2000; Fruneau and Sarti, 2000; Ferretti *et al.*, 2000; Borgia *et al.*, 2000; Ferretti *et al.*, 2001; Le Mouélic *et al.*, 2002; Raucoules *et al.*, 2003a, b).

The purpose of this paper is to present the results of ground deformation for the urban area in the Athens Basin, using the methods of Stacked interferometry and Permanent Scatterers (PS) interferometry. Finally, in an attempt to understand and help to interpret the observed deformation, correlation with other available data (like the distribu-

tion of wells for water pumping, the subway (metro) line tunnelling, the old mining activities, etc.) are examined and discussed.

2. The Athens Basin—A Multi-Parametric Description

The Athens Basin constitutes the largest basin in the Attica Prefecture (Central Greek mainland). The basin is surrounded by the mountains of Aegaleo (468 m), Parnitha (1413 m), Pendeliko (1102 m) and Hymettus (1026 m) (Fig. 1), including a number of small hills distributed within the basin. The southern and south-western part of the basin is open towards the Saronikos Gulf forming a shoreline of about 47 km. Concerning the landuse in the basin, the highland and middle-land zone cover 38% from which 11% corresponds to dense vegetation and 27% to open shrubs. The remaining 62% of the basin is covered by built up area (Antoniou, 2000).

Mining activities, increased water pumping, major underground construction works and large magnitude earthquakes constitute the main sources of ground deformation and subsidence-causes in the broader area of Athens. Old underground mining activities have been taking place in the western part of the basin. The mining (exploitation of lignite) started systematically at the beginning of 1930s up to 1960, and the horizons of excavation were between 50–60 m. Many of the buildings over the mining area, including the new constructions of the urban area, present hairline cracks on the walls. It has been shown that only a part of that area is actually stable, while ground subsidence phenomena are in process in the rest of it (Rosos *et al*., 1999).

The annual water demand in the broader area of Athens had been continuously increasing until the early 1990s. At the same period, persistent drought had caused almost all surface water resources available to be used (Karavitis, 1998). The annual water consumption in the metropolitan area of Athens was about 376×10^6 m³ in 1989, during the last year before the drought period (Karavitis, 1992). The consumption dropped to 326×10^6 m³ during the 1990 drought, and reached a minimum of 246×10^6 m³ in 1993.

Since then it has started to increase, reaching a maximum consumption of 280×10^6 m³ in 1995. During this period municipal and private water drilling were increased to satisfy the demand and overcome the drastic increase of water price. Almost ten years after the end of the drought period, the annual water demand is estimated to be 412×10^6 m³ for the hydrological year 2002–2003 (Koutsogiannis *et al*., 2003).

An intensive program of public and private works was started in early 1990 to improve the facilities in the urban and sub-urban area for the Athens 2004 Olympic Games. Among these works, the new subway with 2 lines in the metropolitan area was one of the most significant and complex projects. About 2,600,000 m³ of excavated rock and soil were produced throughout the excavation work period.

The geological basement of the basin consists of the Athens Schist series extending at a considerable depth, including schists, shales, sandstones, marls and limestones (Koukis and Sabatakakis, 2000). Referring to the younger formations, the basin is locally covered by Tertiary deposits (marls, clays, sandstone and conglomerates), talus cones, alluvial deposits, as well as historic and recent deposits. The neotectonic structure of the broader Athens area comprises a number of major faults with an E-W and NW-SE strike direction. The E-W trending fault system in western Attica is associated with large magnitude earthquakes. On the contrary, the NW-SE trending fault in eastern Attica is related to smaller magnitude tremors (Papanikolaou, 1999).

A large magnitude earthquake ($M_w = 5.9$) occurred at a distance of about 25 km west from the city centre of Athens on September 7, 1999. The epicentre was located south of the Parnitha Mt. in the Thriassio Basin (Fig. 1). The event was the strongest being recorded in this area, which was considered as one of a rather low seismicity (Papadopoulos *et al*., 2000; Papadimitriou *et al*., 2002; Stavrakakis *et al*., 2002). The observed damages were distributed mainly at the northwestern zone of the basin. In these locations, the macroseismic intensity was as high as IX degrees on the modified Mercalli-Sieberg scale, with a local maximum to IX⁺ degrees (Papanastasiou *et al*., 2000). About 100 buildings were collapsed, raising the number of casualties to 143. The damage to lifelines was insignificant, while there were no major ground-failures (liquefactions, slope failures, etc.) triggered by the earthquake (Bouckouvalas and Kourtezis, 2001).

3. Deformation Images

3.1 SAR interferometric techniques

Some of the applications of conventional InSAR measuring ground deformation have already been mentioned. Advanced InSAR techniques have though been developed during the last 5 years that can measure the ground deformation at a millimeter level. These are the PS and the Stacked interferometric techniques. Since the results of this paper are based upon these newly developed techniques, a brief reference to some of their characteristics is also given in the following.

3.2 The PS technique

The PS technique is an advanced processing tool allowing the joint exploitation of series of interferometric SAR
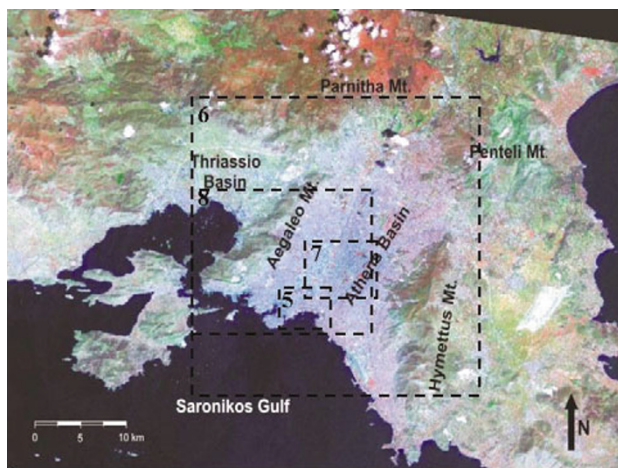

Fig. 1. LANDSAT TM image showing the broader area of Athens Basin, frames 5, 6, 7, 8 delineate the areas covered by the images of the respective figures.

images all referred to a unique master acquisition. This technique was developed at POLIMI (Politecnico of Milano) and its TRE (Tele-rilevamento Europa) commercial spin-off company (Ferretti *et al.*, 2000, 2001, 2004; Colessanti *et al.*, 2003). It involves phase comparison of SAR images, gathered at different times with slightly different looking angles. It has the potential to detect millimetric target displacements along the sensor-target direction (line of sight direction). Geometric decorrelation is due instead to a change in the geometric properties of the two acquisitions (changes in the incidence angle). Temporal decorrelation makes interferometric measurements unfeasible. The use of short revisit times minimizes the temporal decorrelation but slow terrain motion cannot be detected. Geometric decorrelation can be limited when point-wise targets are used (like corner reflectors). In areas affected by either kind of decorrelation, generating the interferogram does not longer compensate reflectivity phase contributions, and possible phase variations due to target motion cannot be highlighted.

The PS approach to overcome limitations due to atmospheric conditions is based on a few basic observations. Atmospheric artifacts show a strong spatial correlation within every single SAR acquisition, but they are uncorrelated in time. Conversely, target motion is usually strongly correlated in time and can exhibit different degrees of spatial correlation depending on the phenomenon at hand (e.g. subsidence due to water pumping, fault displacements, localized sliding areas, collapsing buildings, etc.). Based on these facts, atmospheric effects can be estimated and removed by combining data from long time series of SAR images, such as those available in the ERS archives of ESA, gathering data since late 1991.

As in all differential interferometric applications, results are not absolute both in time and space. Deformation data are referred to the master image (in time) and results are computed with respect to a reference point of known elevation and motion in space. Despite this remark, the PS technique is a sort of natural geodetic network allowing the analyses of surface deformation phenomena over hundreds or thousands of km^2 wide areas. It provides an easy and low cost alternative to traditional monitoring methods like GPS and optical levelling (Colesanti *et al.*, 2001).

The available dataset for the present study comprises 55 ERS1&2 SAR acquisitions. Thirty-eight (38) of them were acquired before the September 7, 1999 earthquake, and 17 after the event. The processing of all the data as a whole with the PS technique can lead to a loss of PS, due to the fact that the reflectivity of the targets can exhibit abrupt changes due to the occurred earthquake. Therefore, the primary dataset was ideally divided into two parts: The pre-seismic and the post-seismic one. Attention was focused on the pre-seismic dataset, made of 38 images spanning the period from May 18, 1992 to August 19, 1999. The processing of the post-seismic dataset is still in progress, as we have to deal with images having Doppler centroid and normal baseline values very high. This makes possible to identify some couple of images to be used for interferogram generation, but it is far more challenging to combine all the images together in order to draw the evolution of the deformation, as the PS technique aims to do.

The PS analysis being focused on the pre-seismic dataset aimed to identify probable precursory motion, as well as other deformation phenomena occurring in the Athens Basin before the major earthquake in 1999. All the images were re-sampled on a common grid defined by the master acquisition, namely the image acquired on March 27, 1997, and 37 differential interferograms referred to this image were computed.

The first step of PS analysis was the identification of a cluster of subset of points, called PS candidates, representing a sparse grid of stable target to be used for the estimation of the atmospheric artefacts (Atmospheric Phase Screen, APS). The information obtained for these points was then extended to the whole image exploiting the low-pass spatial behaviour of the atmosphere. Once the APSs had been estimated, it was possible to remove them from the differential interferograms, so to be able to perform a pixel-by-pixel analysis aimed at the determination of the deformation for each radar benchmark. In this study, the approach used was the so-called Standard PS Analysis, meaning that the deformation model adopted was linear, assuming that the target was moving with a constant velocity over the period 1992–1999. The phase residual obtained with respect to the model used allowed the computation of a quality index, called coherence, providing an indication of the validity of the model and of the reliability of the estimated velocity values. This index is a function mainly of the number of images processed and the dataset distribution (acquisition date and normal baseline values).

Thanks to the high level of urbanisation of the area under analysis, it was possible to identify a huge number of Permanent Scatterers with a high coherence value. About 98000 PS have been identified with coherence greater than 0.8. The information extracted from these points was geo-referenced and incorporated into a GIS environment, which was superimposed on a LANDSAT TM panchromatic image. Ground subsidence rates were then determined adopting the linear character of deformation mentioned above.

The PS interferometric image (Fig. 2) showed an average annual rate of down-lift between 1 to 3 mm/yr in the southern part of the basin, where locally in the City of Piraeus, and the municipalities of Moschato, Kallithea and Nea Smyrni the rate of down-lift increases between 2 to 3 mm/yr. An average annual rate of subsidence from 1 to 2 mm/yr is locally observed within the centre of the basin. Finally, a rate of 3 to 4 mm/yr of down-lift is resulted at the northern part of the basin in the Kifissia area.

3.3 The stacking technique

Stacking differential interferograms involves the summing of multiple differential interferograms into a single interferogram. This is useful to overcome the two shortcomings of conventional InSAR that is the Low Coherence over long temporal separations and the Atmospheric Influence. If reasonable coherence levels can only be obtained over short time periods, as for example in the case of rural settings in temperate climates, then several short time periods, temporally contiguous interferograms can be summed (subject to data availability) to produce a pseudo-interferogram over a longer period. This enables low magnitude displacements to be monitored over longer periods, where no single
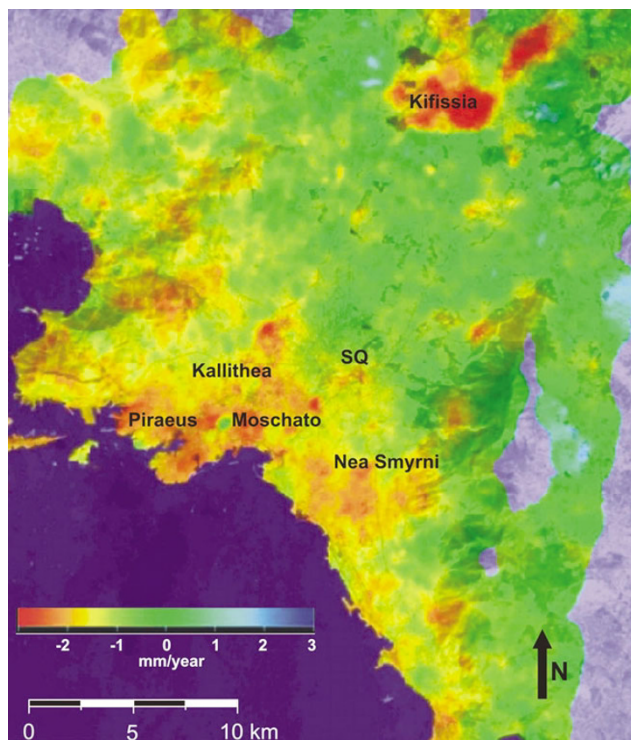
Fig. 2.   PS Interferometric Image of the Athens Basin for the period 1992–1999. The yellow and reddish colors represent areas undergoing to down-lift, while the cyan and bluish colors areas of up-lift. SQ: Syntagma Square.
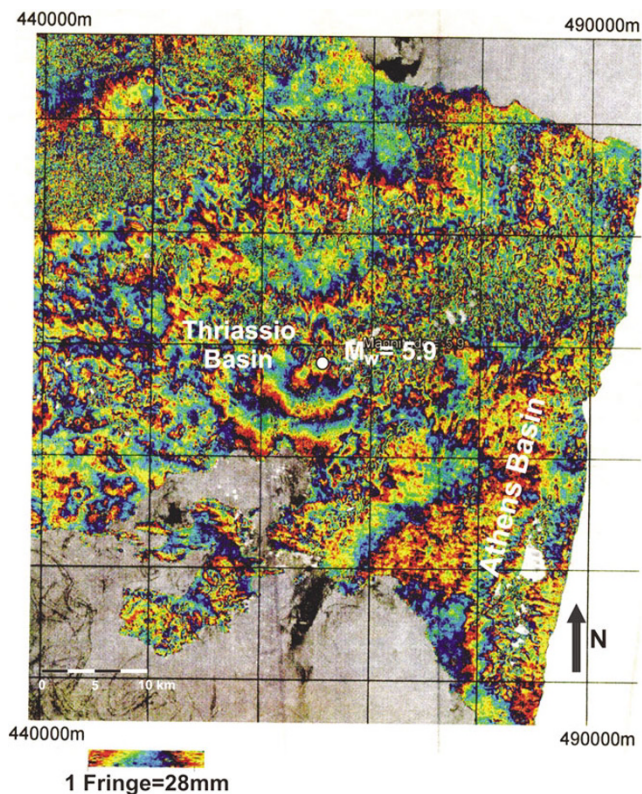

Fig. 3. InSAR image, of September 7 1999 earthquake event ($M_w = 5.9$), showing fringe deformation pattern in the broader area of Athens. The inner fringe in Thriassio Basin corresponds to maximum deformation of 3×28 mm along the line of sight and coincides with the earthquake epicenter (white circle) area.

coherent interferogram exists.

Regarding atmospheric influences, when multiple differential interferograms exist bracketing an instantaneous event (such as an earthquake event or other sudden ground displacement), they can be summed to increase the (displacement) signal to (atmospheric) noise ratio. This is possible because the displacement signal is constant in each interferogram, whereas the atmospheric signal varies randomly. With specific topographic characteristics (Delacourt *et al.*, 1998) atmospheric effetcs can have a certain temporal correlation. The averaging effect could be therefore less effective that a 1/sqrt (N) improvement of the inaccuracy. Notice that such a drawback would also affect any InSAR processing based on the low temporal correlation of the atmospheric signal, including PSInSAR techniques.

In the case of non instantaneous (for example linear) deformation, summing interferograms on equivalent periods (approximately same start and end dates) will also reduce the atmosphere/deformation ratio and the obtained pseudo-interferograms will have an increased accuracy respect to initial ones. Addition of interferograms of successive periods can also allow retrieving a deformation on the whole period covered by the data. If the deformation is continuous on the cumulated period, the deformation component will be also enhanced respect to atmosphere. In both cases a previous interpretation of the interferograms is needed in order to select the ones to be added (preferably without excessive atmospheric effects on the spotted deformation signatures). In particular for the smaller deformation signatures, the main element to confirm that the observed signature is

not related to atmosphere is the persistence of the signature on different independent interferograms. The computational effort required to stack interferograms is limited, once the interferograms themselves have been produced. However, such a strategy can only be applied to the selected circumstances described above. Also, an understanding of the temporal evolution of the deformation is desirable to determine if interferogram stacking is relevant. This generally means that a previous interpretation of the interferogram series would be required before stacking is considered (Strozzi *et al.*, 2001; Raucoules *et al.*, 2003b).

Implementing the stacking technique, the 55 SAR available images were processed in order to produce 264 interferograms applying an automated procedure based on IDL image processing software and on the Gamma interferometric software. All the possible combinations with baselines less than 200 m were computed. The topographic component was removed using a 50 m × 50 m sampling DEM that was re-sampled to 25 m × 25 m. Between these 264 interferograms, a set of 60 interferograms was selected for their quality in terms of high coherence and low noise level. These interferograms were filtered using an adaptive filter (Goldstein and Werner, 1998) to reduce their noise. A first visual interpretation was carried out in order to identify the main deformation signatures.

The construction of the co-seismic differential interferogram, using an interferometric pair composed by two ERS-2 SAR images covering the period 15-7-99/23-9-99 with
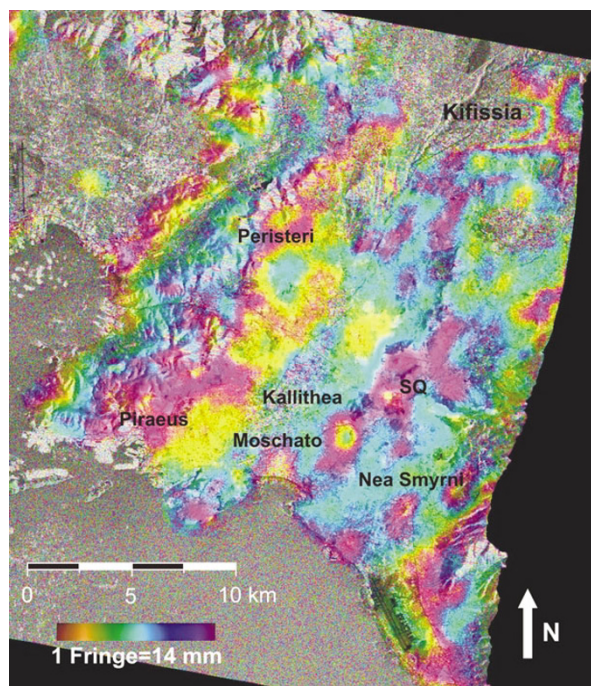
Fig. 4. Interferometric Stacking Image of the Athens Basin for the period 1992–2002. The sequence of colors in the scale-bar represents 0–2 p rad phase variation, equal to one fringe (=14 mm) of displacement in the direction opposed to the sensor. SQ: Syntagma Square.

Bperp = 133 m, associated with the Athens 1999 major earthquake was made (Fig. 3). It can be seen that a wide-scale of deformation pattern consisting of almost 3 fringes (1 fringe = 28 mm) related to the earthquake occurrence was identified. The deformation is primarily located in the adjacent basin of Thriassio at the west of Athens basin and secondarily at the northwestern part of Athens basin. Previous studies for mapping the co-seismic deformation of the same seismic event were also carried out (Kontoes *et al.*, 2000; Parcharidis and Foumelis, 2005). The results, including spatial distribution of deformation, of these studies are consistent with the present one, even though different spanning periods of SAR pairs were used.

The analysis of the present study was focused on interferometric pairs that do not overlap with the earthquake event; the co-seismic deformation associated with the tremor was thus excluded. The formed interferograms contain information of aseismic deformation only. Several sums of interferometric phases of different independent pairs covering the same period were produced. This stacking process enhances deformation signatures with respect to atmospheric effects. The sum of pairs covering successive periods was also computed to provide long time span pseudo interferograms on a time span that could not be reliably covered by a single interferogram due to coherence loss.

The linear combination (in this case a sum) of four interferograms covering the periods (i) 1992-05-18/1998-12-17, (ii) 1992-08-31/1997-11-27, (iii) 1999-09-23/2001-11-01 and (iv) 2000-12-21/2002-07-04, resulted in the formation of a pseudo-interferogram spanning the period 1992–2002, where the co-seismic signature of the Athens Earthquake (1999-09-07) was excluded. This pseudo-interferogram

(Fig. 4) reveals a total deformation signature of less than one fringe in the southern part of the basin (fringe = 14 mm obtained assuming a linear deformation and taking into account the time spans of each interferogram). That is in Moschato and Kallithea municipalities, a subsidence of about 12 mm is observed. Also, the city centre of Athens in the vicinity of Syntagma Square, and the Municipality of Nea Smyrni appear to have smaller amplitude of subsidence, about 10mm, since a not fully formed fringe is observed in these areas. Note that the amount of about 10 mm is close to the precision of the method (7–10 mm). In the northeastern area of Athens Basin and specifically in Kifissia area, a number of less than 3 fringes of deformation are observed. Greater values of subsidence of at least 40 mm are therefore measured in this area.

From the co-seismic intrferogram (Fig. 3) ground deformation is detected in NW part of Athens basin. However, in the stacking interferogram that partially covers the post seismic period there is no any evident deformation pattern in this area. Additionally, from the stacking image the areas that show deformation are the southern and eastern parts of the basin. Due to these reasons it is assumed that the deformation presented in the stacking image is not related to the seismic and post seismic events.

4. Correlation with Other Data

Other available data were also considered to help to interpret the deformation images. These data are related to the geology (lithology and tectonics), seismicity (spatial distribution of the earthquake epicentres), hydrogeology (drainage network, watershed boundaries and boreholes for water pumping), areas of old mining activities, and subway-line spatial distribution. The data being in a raster and vector forms were geo-referenced and imported together with the deformation images into a GIS platform for an easier manipulation. Additionally, the following very high-resolution satellite data were used: (i) A Panchromatic image of IRS Indian satellite with pixel resolution of 5.5 m, covering the entire Athens Basin with 5% cloud coverage. (ii) A QUICKBIRD image: (four spectral bands 4 m/pixel and panchromatic 0.7m/pixel) cloud-free image, covering the central part of the City of Athens.

An attempt to investigate the correlation of the spatial distribution between the observed deformation patterns in the two interferometric images (Figs. 2 and 4) and a number of potential sources, like geological and man-made parameters, was carried out. The ARC-View software was used to superimpose deformation images with raster and vector thematic layers. The spatial correlation between the horizontal extent of the observed deformation and some of the possible potential sources are examined in the following.

Local Geology: The geological parameters of the Athens Basin show that the deformation observed in Moschato area may be attributed to the existing lithology in the area. The deformation is observed in both images (Figs. 5(a) and (b)) and it is estimated 2 to 3 mm/year for the PS and 12 mm for a period of 9 years for the stacking data. In this case a small divergence of the deformation rates in the two images concerning the quantitative estimation of the local deformation is observed. Specifically, the Moschato area is
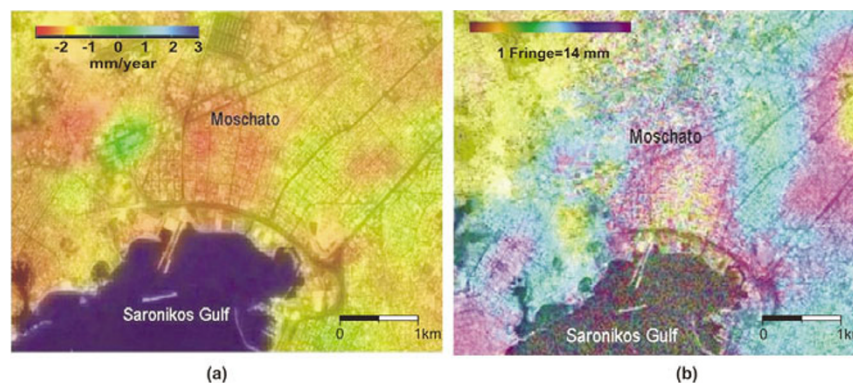
Fig. 5. Deformation Pattern of the southern part of the Athens Basin applying (a) the PS Technique, and (b) the Stacking Technique.
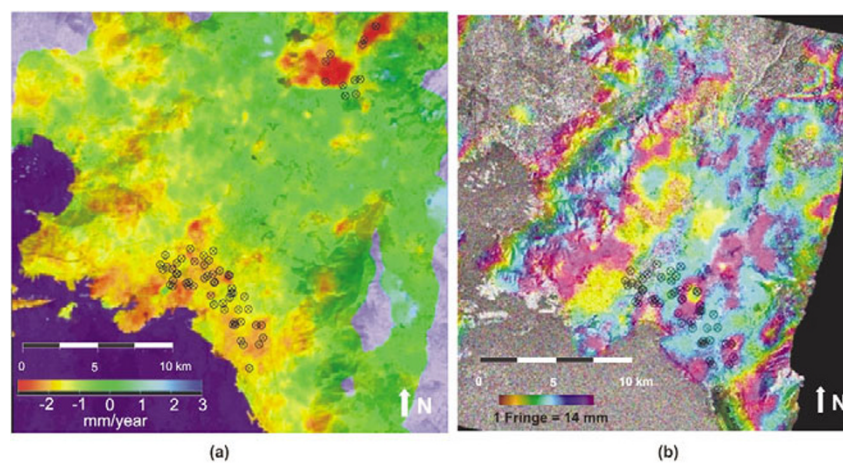

Fig. 6. Water well locations (showed as ⊗): (a) of the PS Interferometric Image, and (b) of the Stacking Interferometric Image in the Athens Basin.

covered by alluvial and marshal deposits, both being deposited in Holocene times by the two main rivers, Kifissos and Ilissos. The area between the two deltas was a swamp until historical times, when it was drained. Marshal deposits consist mostly of clay organic material, and their thickness may be up to 5 m. Alluvial deposits consist mainly of clay, sands, and a few conglomeratic intercalations. Their thickness may reach up to 30 m. Concerning the morphology, the area is flat and at a sea-level altitude and suffers by flash floods during the winter. Regarding the spatial correlation between the observed deformation and the existing fault systems, there is no evident correlation in the margins of the basin, or within the building area.

Water Wells. The spatial distribution of the well drillings for water supply (only those official drillings carried out by the local authorities are presented here) shows a good correlation with the deformation pattern in the PS interferometric image in the southern area, as well as in the northeastern one (Fig. 6(a)). Referring to the stacking results, no evident correlation is observed in the southern part; however, a very good correlation is observed in the northeastern area (Fig. 6(b)). The rate of deformation, in the northern area, detected by the two techniques is similar that is 3 to 4 mm/year for PS and 40 mm for the 9 years covered by the stacking technique. It is though worth mentioning here that the number of water drillings in the northern part is greater than in the southern part due to existence of a large number of private drillings. The latter could explain the larger extension of the deformation pattern in both interferometric images.

Tunneling Activities. Superposition of the metro tunnel paths on the measured deformation (Fig. 7) shows that there is not any significant consequence in the amplitude and horizontal extent of the observed deformation pattern. Regarding the results of the PS technique along the two metro lines, it appears that there is not any evident correlation with the exception for the area around the Acropolis metro station (Fig. 7(a)), where the deformation corresponds to about 1 to 2 mm/year. The pattern of deformation in the area is not elongated following the tunnel path, but exhibits a spatial distribution around the metro station. The Acropolis metro station is of a particular importance, since it is closer to the Acropolis Hill and the historical centre of Athens. The largest deformation pattern is observed at the Syntagma metro station (Fig. 7(a)), the spatial distribution of which only partially coincides with the extension of the station itself. Comparing the resulted deformation using the stacking technique with the metro tunnel path (Fig. 7(b)), it can be seen that there is a high spatial correlation between the Syntagma metro station and the pattern of a not fully formed fringe, corresponding to about 10 mm.

Mining Activities. The old mining area (working period 1930–1960) is located in the western part of the basin (Peristeri), which is actually a densely populated area. Referring
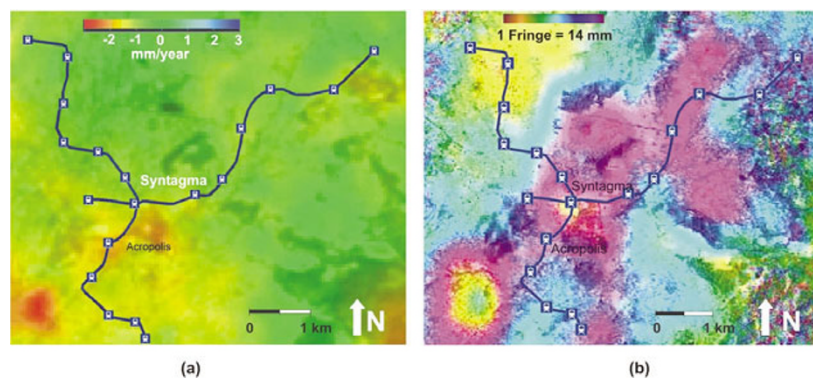
Fig. 7. Lines and stations of metro subway overlapping the (a) PS Image, and (b) the Stacking Image.
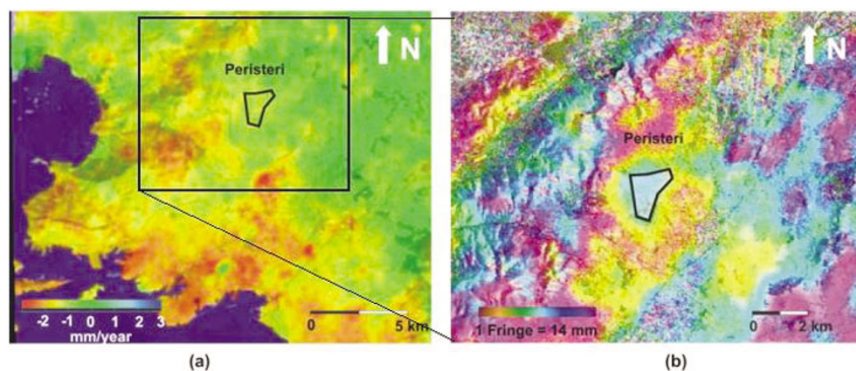

Fig. 8. Spatial extension of old mining area (shown as a polygon line) located at the western part of the Athens Basin overlapping the PS Image (a), and the Stacking Image (b).

to the PS results, there is not any clear correlation. The broader area shows a deformation rate of 1 to 2 mm/year (Fig. 8(a)). Regarding the stacking results, there is a clear correlation between the fringe pattern and the contour encompassing the mining area (Fig. 8(b)). The detected deformation (subsidence) is about 14 mm. The former observation is supported by internal reports of the Institute of Geology and Mining Exploration (IGME) in Athens, where it is reported that hair-type openings were observed at the buildings in the zone above the old mines during the '90s.

5. Discussion—Conclusions

Conventional InSAR and PS analysis was possible to be carried out on a set of ESA-ERS satellite images acquired over the broader area of Athens. The detection of unstable areas and some measurement of the local dynamics were also achieved. Even though classical interferometry may face major problems due to temporal and geometrical decorrelation, nevertheless, some motion information was extracted for fast and local deformation phenomena in coherent areas. Consistent results were achieved by adopting recent multi-interferogram strategies, such as the Stacking and the PS techniques.

A major limitation of the PS approach, common to all InSAR techniques, could be the density of the measurement points. The number of PS and the average coherence level for interferogram stacking were high enough to properly measure local motion. PS results show that the northeastern part of the basin subsides with faster rates (3 to 4 mm/yr)

than the southern margin (1 to 3 mm/yr), while a rate of 1 to 2 mm/yr is measured at about the centre of the basin and the city centre (Syntagma Square). A subsidence rate of 1 to 2 mm/yr is identified at the western part of the basin.

Stacking results yield amplitude of subsidence over a period of approximately 9 years. A subsidence of 40 mm is measured at the northeastern part (Kifissia area) consistent with the annual rate of the PS results. However, a lower level of subsidence (12 mm) is locally observed in Moschato and Kallithea at the southern part compared to the rate (2 to 3 mm/yr) exhibited by PS. In the city centre, the amplitude ($\sim$10 mm) determined by stacking corresponds to the lower PS rate limit (1 to 2 mm/yr). A well-identified fringe pattern corresponding to 14 mm of subsidence is located at the western part of the basin (Peristeri) marking the area of the old mining activities in a much clearer manner compared to the PS.

It appears that the subsidence observed at the northeastern part (Kifissia area) may be attributed to intense water pumping from a large number of public and private wells. The same cause should be considered at the southern part (Moschato and Kallithea), but to a lesser extent, since the local geology characteristics most probably contribute to those subsidence effects. Confidence may be expressed at the western part (Peristeri), where the noticed subsidence effects are associated with the older underground mining activities. Finally, it has to be mentioned that the observed subsidence around the area of Syntagma Square encompasses a much larger area than that associated with the un-

derground construction of metro lines and stations.

Significant research efforts should be devoted in the future to the design and the reliable installation of artificial reflectors (or to study PS density as a function of frequency and/or polarization) in order to increase the spatial sampling of the phenomena under study. Successful probability of a full PS processing (related to PS density) can often be estimated in advance from an analysis of high resolution optical data relative to the area under study (the density of buildings and rocky area is proportional to PS density). Also, when considering some a priori information about the displacement rate of surface deformation phenomena; it is enough to know whether the expected line of sight (LOS) motion is less than 4–5 cm/yr.

Interferogram stacking have provided interesting additional information on areas affected by sudden deformation or deformation with large amplitudes, as in the case of the Athens tremor, whereas the PS technique was less efficient. Since SAR multi-temporal analysis allows the estimate of high-accuracy relative vertical displacements over wide areas at low cost, synergistic strategies with GPS networks should be applied for seismological studies and monitoring of tectonic motion.

Integration of all available data in a GIS environment found to be extremely useful to provide decision makers with all the information needed. The identification of all the specifications and the constraints of a Decision Support System for surface deformation monitoring is out of the scope of this study; however, it deserves a special attention. For Civil Protection applications, the detection of the surface deformation phenomena, especially related to landslides, mining activities, as well as seismic faults, can be of outmost importance. Thus, provided that PS are available (be they natural or artificial) on the area under study, deformation occurring during the creeping, pre-rupture phase of a potentially dangerous landslide could be timely detected, allowing one to undertake subsequent actions. This is probably the most important aspect inferred by the potential of the applied techniques of this study.

References

Amelung, F., D. Galloway, J. Bell, H. Zebker, and R. Laczniak, Sensing the ups and downs of Las Vegas: InSAR reveals structural control of land subsidence and aquifer-system deformation, *Geology*, **27**, 483–486, 1999.

Antoniou, B., The geo-environmental conditions of Athens Basin, Doctorate Thesis (in Greek), Agriculture University of Athens, Greece, 2000.

Avallone, A., P. Briole, C. Delacourt, A. Zollo, and F. Beauducel, Subsidence at Campi Flegrei (Italy) detected by SAR interferometry, *Geophys. Res. Lett.*, **26**, 2303–2306, 1999.

Borgia, A., R. Lanari, E. Sansosti, M. Tesauro, P. Berardino, G. Fornaro, M. Neri, and J. B. Murray, Actively growing anticlines beneath Catania from the distal motion of Mount Etna's devolvement measured by SAR interferometry and GPS, *Geophys. Res. Lett.*, **27**(20), 3409–3412, 2000.

Bouckouvalas, G. and G. Kourtezis, Stiff soil amplification effects in the September 7, 1999, Athens (Greece) earthquake, *Soil Dynamics and Earthquake Engineering*, **21**, issue 8, 671–687, 2001.

Carnec, C. and C. Delacourt, Three years of mining subsidence monitored by SAR interferometry, Gardanne, France, *Applied Geophysics*, **43**, 43–54, 2000.

Carnec, C. and H. Fabriol, Monitoring and modeling land subsidence at the Cerro-Prieto geothermal field, Baja California, Mexico, using SAR interferometry, *Geophys. Res. Lett.*, **9**, 1211–1214, 1999.

Colesanti, C., A. Ferretti, C. Prati, and F. Rocca, Comparing GPS, Optical Levelling and Permanent Scatterers, *Proc. IEEE International Geoscience and Remote Sensing Symposium—IGARSS 2001*, Sydney, Australia, 9–13 July, 6, 2622–2624, 2001.

Colessanti, C., A. Ferretti, C. Prati, and F. Rocca, Monitoring landslides and tectonic motion with the permanent scatterers technique, *Engineering Geology*, **68**, 3–14, 2003.

Delacourt, C., P. Briole, and J. Achache, Tropostpheric corrections of SAR interferograms with strong topography. Application to Etna, *Geophys. Res. Lett.*, **25**(15), 2849–2852, 1998.

Ferretti, A., F. Ferrucci, C. Prati, and F. Rocca, SAR analysis of building collapse by means of the permanent scatterers technique, *Proc. IEEE International Geoscience and Remote Sensing Symposium—IGARSS 2000*, Honolulu, USA, 24–28 July 2000, 7, 3219–3221, 2000.

Ferretti, A., C. Colesanti, C. Prati, and F. Rocca, Radar Permanent Scatterers Identification in Urban Areas: Target Characterization and Sub-Pixel Analysis, *Proceedings of the Joint IEEE/ISPRS Workshop on Remote Sensing and Data Fusion over Urban Areas, Roma, Italy*, 8–9 November 2001, 52, 2001.

Ferretti, A., F. Novali, R. Bürgmann, G. Hilley, and C. Pratti, InSAR Permanent Scatterer analysis reveals ups and downs in San Francisco Bay area, *EOS, Transactions, AGU*, **85/34**, 317–324, 2004.

Fielding, E. J., R. G. Blom, and R. M. Goldstein, Rapid subsidence over oil fields measured by SAR Interferometry, *Geophys. Res. Lett.*, **25**, 3215–3218, 1998.

Fruneau, B. and F. Sarti, Detection of Ground Subsidence on the city of Paris using Radar Interferometry: Isolation, of deformation from atmospheric artifacts using correlation, *Geophys. Res. Lett.*, **28**, 3981–3984, 2000.

Galloway, D. L., K. W. Hudnut, S. E. Ingebritsen, S. P. Phillips, G. Peltzer, F. Rogez, and P. Rosen, Detection of aquifer system compaction and land subsidence using interferometric synthetic aperture radar, Antelope Valley, Mojave Desert, California, *Water Resources. Res.*, **34**, 2573–2585, 1998.

Goldstein, R. and C. Werner, Radar interferogram filtering for geophysical applications, *Geophys. Res. Lett.*, **21**, 4035–4038, 1998.

Hoffmann, J., H. A. Zebker, D. L. Galloway, and F. Amelung, Seasonal subsidence and rebound in Las Vegas Valley, Nevada, observed by synthetic aperture radar interferometry, *Water Resources Res.*, **37**, 1551–1566, 2001.

Karavitis, C. A., Drought management strategies for urban water supplies: The case of metropolitan Athens, Ph.D. Thesis, Dept. Civil Engin., Colorado State University, USA. 1992 (in Greek).

Karavitis, C. A., Drought and urban water supplies: The case of Metropolitan Athens, *Water Policy*, **1**, 505–524, 1998.

Kontoes, C., P. Elias, O. Sykioti, P. Briole, D. Remy, M. Sachpazi, G. Veis, and I. Kotsis, Displacement field and fault model for the September 7, 1999 Athens earthquake inferred from ERS2 satellite radar interferometry, *Geophys. Res. Lett.*, **24**, 3989–3992, 2000.

Koukis, G. and N. Sabatakakis, Engineering geological environment of Athens, Greece, *Bull. Eng. Geol. Env.*, **59**, 127–135, 2000.

Koutsogiannis, D., G. Karavokiros, A. Efstratiadis, N. Mamassis, A. Koukouvinos, and A. Christofides, A decision support system for the management of the water resource system of Athens, *Physics and Chemistry of the Earth*, **28**, 599–609, 2003.

Le Mouélic, S., D. Raucoules, C. Carnec, C. King, and F. Adragna, A ground uplift in the city of Paris (France) detected by satellite radar interferometry, *Geophys. Res. Lett.*, **29**, 1853, 2002.

Massonnet, D., M. Rossi, C. Carmona, F. Adragna, G. Pelmtzer, K. Feigl, and T. Rabaute, The displacement field of the Landers Earthquake mapped by radar interferometry, *Nature*, **364**, 138–142, 1993.

Papadimitriou, P., N. Voulgaris, I. Kassaras, G. Kaviris, N. Delibassis, and K. Makropoulos, The M_w = 6.0 September 7, 1999, Athens Earthquake, *Natural Hazards*, **27**(1), 15–33, 2002.

Papadopoulos, G., G. Drakatos, D. Papanastassiou, I. Kalogeras, and G. Stavrakakis, Preliminary results about the catastrophic earthquake of 7 September 1999 in Athens, Greece, *Seismol. Res. Lett.*, **71**, 318–329, 2000.

Papanastasiou, D., D. Stavrakakis, G. Drakatos, and G. Papadopoulos, The Athens September 7, 1999, Ms = 5.9 earthquake: First results on the focal properties of the main shock and the after shock sequence, *Annales*

Geologiques des pays Helleniques, **38b**, 73–88, 2000.

Papanikolaou, D., Geology and tectonics of western Attica in relation to the 7-9-1999 earthquake, *Newsletter of the European Centre on Prevention and Forecasting of Earthquakes*, **3**, 30–34, 1999.

Parcharidis, Is. and M. Foumelis, On the Assessment of Co-Seismic InSAR Images of Different Time Span Associated to Athens (Greece) 1999 Earthquake, *IGARSS 2005*, **7**, 5251–5254, 2005.

Raucoules, D., S. Le Mouélic, C. Carnec, C. Maisons, and C. King, Urban subsidence in the city of Prato (Italy) monitored by satellite radar interferometry, *Intern. J. Remote Sensing*, **24/4**, 891–897, 2003a.

Raucoules, D., C. Maisons, C. Carnec, S. Le Mouélic, and C. King, Accurate monitoring of slow ground deformation by ERS radar interferometry—The case of Vauvert (France), *Remote Sensing of Environment*, **88**(4), 468–478, 2003b.

Rosos, D., I. Vakondios, M. Kinygalaki, and Ch. Argyri, Geotechnical study of the ground subsidence in Peristeri area, Athens, Technical Report, Institute of Geology and Mineral Exploration (IGME), Athens, Greece, 1999.

Stavrakakis, G., G. Chouliaras, and G. Panopoulou, Seismic source parameters for the $M_L = 5.4$ Athens earthquake, September 7, 1999, from a new telemetric broad band seismological network in Greece, *Natural Hazards*, **27**(1), 47–60, 2002.

Strozzi, T., U. Wegmüller, L. Tosi, G. Bitelli, and V. Spreckels, Land subsidence monitoring with differential SAR interferometry, *Photogrammetric Engineering and Remote Sensing*, **67**, 1261–1270, 2001.

Tesauro, M., P. Berardino, R. Lanari, E. Sansisti, G. Fornaro, and G. Franschetti, Urban subsidence inside the City of Napoli (Italy) observed by satellite radar interferometry, *Geophys. Res. Lett.*, **27**, 1961–1964, 2000.

Wegmüller, U., T. Strozzi, and G. Bitelli, Validation of ERS differential SAR interferometry for land subsidence mapping: the Bologna case study, *Proc. IGARSS'99, Hamburg, Germany*, 28 June–2 July, 1999.

Wright, P. and R. Stow, Detecting mining subsidence from Space, *Int. J. Remote Sensing*, **20/6**, 1183–1188, 1999.

Zebker, H. A., P. A. Rosen, R. M. Goldstein, A. Gabriel, and C. L. Werner, On the derivation of coseismic displacement-fields using differential radar interferometry: the Landers earthquake, *J. Geophys. Res., Solid Earth*, **99**(B10), 19617–19634, 1994.

Is. Parcharidis (e-mail: parchar@hua.gr), E. Lagios (e-mail: lagios@geol.uoa.gr), V. Sakkas (e-mail: vsakkas@geol.uoa.gr), D. Raucoules (e-mail: d.raucoules@brgm.fr), D. Feurer, S. Le Mouelic, C. King, C. Carnec, F. Novali (e-mail: Fabrizio.novali@treuropa.com), A. Ferretti (e-mail: alessandro.ferretti@treuropa.com), R. Capes (e-mail: ren@npagroup.com), and G. Cooksley (e-mail: Geraint@npagroup.com)